Avens Publishing Group
J Environ Stud
October 2020 Vol.:6, Issue:1

Open Access Research Article

Journal of Environmental Studies

Remediation of Contaminated Water With Crystal Violet Dye by Using Magnetite Nanoparticles: Synthesis, Characterization and Adsorption Mechanism Studies

Abobakr SM[1], Abdo NI[2*] and Mansour RA[1]

[1]*Higher Institute of Engineering and Technology, New Damietta, Egypt*
[2]*Higher Institute of Engineering and Technology, New Borg Al Arab, Egypt*

***Address for Correspondence**
Abdo NI, Higher Institute of Engineering and Technology, New Borg Al Arab, Egypt; E-mail: nabiha_ibrhim@yahoo.com

Submission: 14 September, 2020
Accepted: 28 October, 2020
Published: 30 October 2020

Keywords: Dye removal; Magnetite nanoparticles (MNPs); TEM; FT-IR; Adsorption mechanisms; Freundlich isotherm

Abstract

Magnetite Nanoparticles (MNPs) have become a promising material for scientific research. Among numerous technologies, MNPs seem to be one of the most convenient to environmental applications as adsorbent. In the present study, the dye adsorption from aqueous solution, using available resources such as Crystal Violet (CV) as model colorant was used. The magnetic nanoparticles (MNPs: before and after adsorption) were characterized by FTIR, SEM and TEM techniques. These nanoparticles have a spherical shape and their diameter about 11nm. The influence of several experimental conditions (pH, contact time, sorbent dose, concentration and temperature) as well as properties of the adsorbent materials in terms of thermodynamics, kinetics and adsorption isotherms was all investigated. Once compared with adsorption models, our results enabled us to describe this adsorption as a process being spontaneous, exothermic and having pseudo-second order kinetics. The adsorption isotherm data were described by the Freundlich model.

Introduction

Dyes are known as pollutants that not only affect aesthetic advantages of environment, but also reduce light penetration and photosynthesis, and some of them are considered toxic and even carcinogenic to human health [1]. Adsorption process provides an attractive alternative for the treatment of colored wastewaters due to its simplicity, selectivity, and efficiency [2-6].

Recently, Adsorbents with magnetic properties such as MNPs have attracted interest in many environmental engineering related applications due to a significant effect in accelerating separation and improving the efficiency of water treatment. With reported sizes ranging from 1 to 100 nm, high surface-to-volume ratio, and high loading capacity, MNPs were successfully used as adsorptive materials for pollutants [7-9]. Therefore, these nanoparticles received significant attention as a low-cost processing and operational easiness adsorbents for potential applications in the environmental treatment.

CV dye is highly toxic to mammalian cells and could cause skin and digestive tract irritation. Also, It may leads to respiratory and kidney failure in extreme conditions. Thus it is necessary to remove this dye from waste water before its final disposal.

The study scope is to investigate the adsorption behavior of MNPs as a surfactant for removal of crystal violet (CV). Based on this, the effects of variables influencing the removal of dyes were evaluated. The adsorption kinetics and isotherms for CV dye onto MNPs were studied.

Experimental

Materials

Crystal Violet ($C_{25}H_{30}N_3Cl$) as a cationic azo dye, ferric chloride ($FeCl_3.6H_2O$), ferrous sulfate ($FeSO_4.7H_2O$), ammonium hydroxide (NH_4OH), diluted hydrochloric acid (HCl) and sodium hydroxide (NaOH) were used for this study. A stock solution of CV (1000 mg l^{-1}) was prepared in distilled water. This solution was diluted with distilled water to prepare stock solutions with the concentration of 10, 25 and 50 mg l^{-1} of CV.

Preparation of magnetite nanoparticles (MNPs)

Stock solutions of ferrous ions (Fe^{+2}; 1M) and ferric ions (Fe^{+3}; 2M) were prepared by dissolving appropriate weight in 200 ml of distilled water, the stock solutions were mixed and heated at 90 ˚C, ammonium hydroxide solution (33%) was introduced by syringe dropwise until pH adjust around 10-12. The appearance of black colour was indicated the formation of magnetite particles. The black mixture was heated at 80 ˚C for 60 minutes, filtered and washed with deionized water repeatedly until pH become neutral and dried at room temperature [10].

$$Fe^{2+} + 2Fe^{3+} + 8NH_3.H_2O \rightarrow Fe_3O_4 + 8NH_4^+ + 4H_2O$$

Preparation of crystal violet dye solution

A stock solution of CV (1000 mg/l) was prepared by dissolving 1 gm in 1 liter distilled water. Then, it diluted by distilled water to prepare different concentrations of dye according to dilution law.

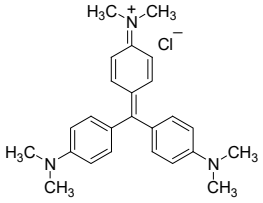

Citation: Abobakr SM, Abdo NI, Mansour RA. Remediation of Contaminated Water With Crystal Violet Dye by Using Magnetite Nanoparticles: Synthesis, Characterization and Adsorption Mechanism Studies. J Environ Stud. 2020;6(1): 10.

ISSN: 2471-4879

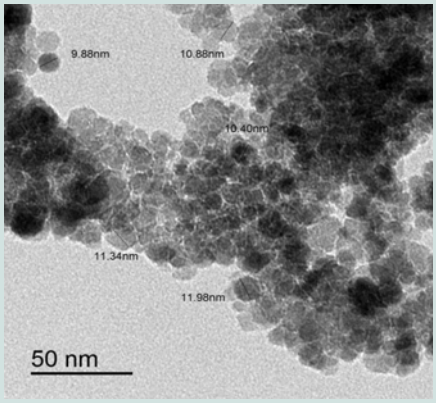

Figure 1: TEM micrograph of pure MNPs.

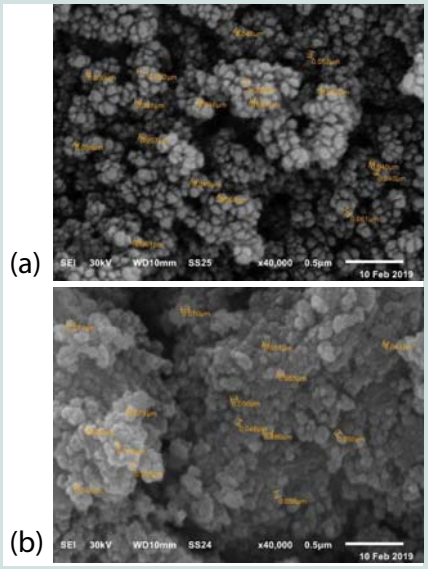

Figure 2: SEM micrographs: (a) Pure MNPs before adsorption; (b) MNPs after adsorption of CV.

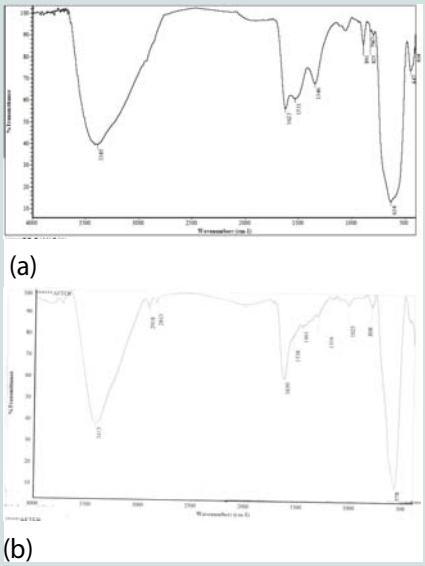

Figure 3: FT-IR: (a) Pure MNPs before adsorption; (b) MNPs after adsorption.

ISSN: 2471-4879

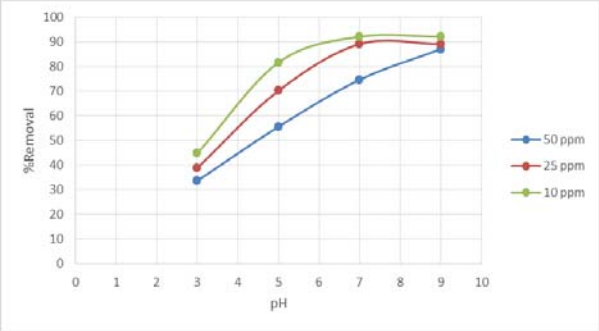

Figure 4: Influence of pH on the adsorption of CV by MNPs. (Dosage 1.8 g, 35 min contact time and room temperature).

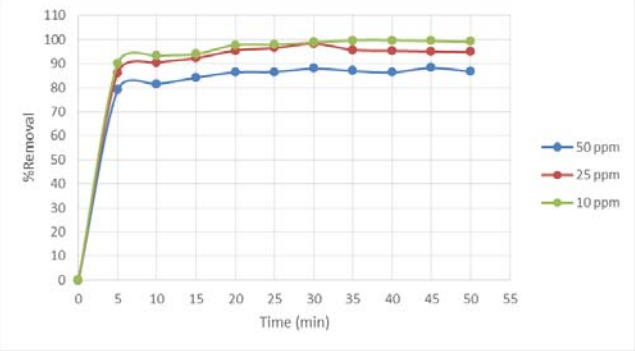

Figure 5: Influence of time on the adsorption of CV by MNPs. (Dosage 1.8 g and room temperature).

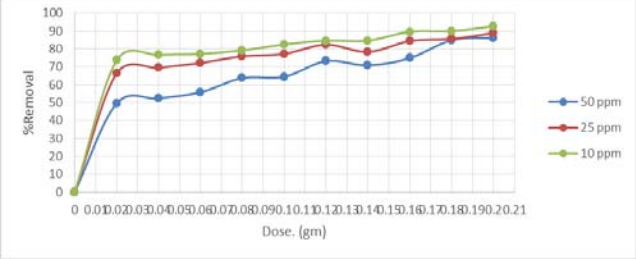

Figure 6: Influence of sorbent dose on the adsorption of CV by MNPs. (35 min contact time and room temperature).

The dye was made up in stock solution of concentration 1000 mg l^{-1} (1 g CV in 1000 ml of distilled water) and was subsequently diluted to the required concentrations from 10 to 100 mg l^{-1}. The effect of some parameters such as pH (3-9) and adsorbent dosage (0.02-0.2 g) was made by known amount of MNPs and 25 ml of CV solution. The pH of dye solution was adjusted using with 0.1 M HCl or 0.1 M NaOH solutions. The sorption studies were performed at different temperatures (25 °C-95 °C). The mixture was shaken using water bath at 240 rpm (25 °C for 30 min). After each adsorption process, the residual CV solution was separated the absorbance of the filtrate was measured at λ_{max} 576 nm. In all these different parameters, the amount of dye taken by adsorbent is calculated as:

$$q_e = (C_i - C_e)\ v/m \quad (15)$$

Where: (q_e; the amount of dye taken by adsorbent (mg/g)), (C_i and C_e; the concentrations of dye at initial and equilibrium (mg/l), respectively), (V; the volume of solution (l)) and (m; the mass of adsorbent (g)). Also the removal efficiency is calculated as:

$$\%Removal = (C_i - C_f)/Ci * 100 \quad (16)$$

Where: (C_i and C_f: the initial and final dye concentrations (mg/l), respectively).

Characterization

FT-IR spectra of the samples were carried out using (FT/IR-4100) spectrophotometer (ThermoFisher Nicolet IS10, USA) in KBr pellets at room temperature. Micrographs of the samples were taken using SEM (JSM-6510, JEOL, Ltd.). The images of TEM were taken by a JEM-2100 operated at an accelerating voltage of 200 kV. UV-visible spectroscopic analysis was carried out on Oasis Scientific (PG Instruments T80).

ISSN: 2471-4879

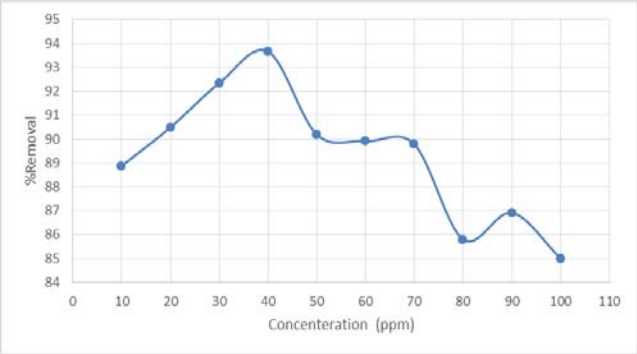

Figure 7: Influence of dye concentration on the adsorption of CV by MNPs. (Dosage 1.8 g, 35 min contact time and room temperature).

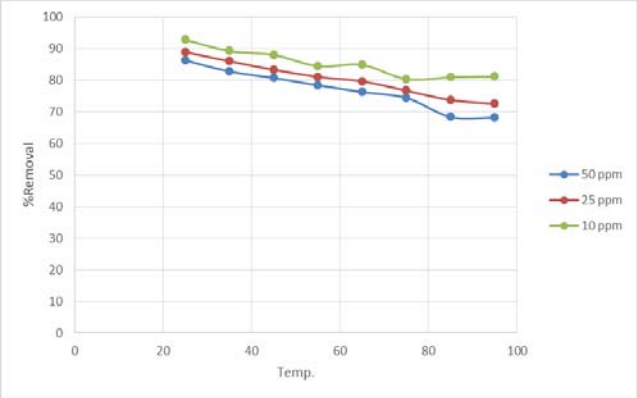

Figure 8: Influence of temperature on the adsorption of CV by MNPs. (Dosage 1.8 g, 35 min contact time).

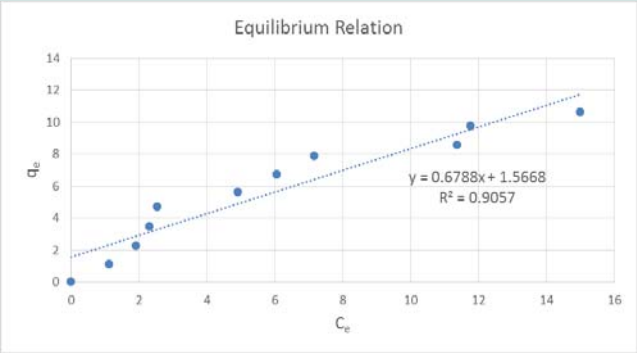

Figure 9: Equilibrium relation between Ce and qe.

Results and Discussion

Morphology Characterization

The morphology and particle size of the prepared MNPs was investigated by TEM. As shown in Figure 1, MNPs exhibited spherical morphologies with a uniform particle size (about 11 nm).

The morphologies of MNPs (a: before adsorption) and MNPs-CV (b: after adsorption) are investigated by SEM and shown in Figure 2. It can be seen from this Figure 2 (2a) that MNPs shows a spherical shape with aggregated porous surface, but MNPs-CV (2b) has a relatively loose and fibrous surface, which indicated the penetration of dye molecules into the MNPs powder.

The FT-IR spectra of Fe_3O_4 before and after adsorption were shown in Figure 3. The presence of strong broad absorption band at around 447- 634 cm^{-1} shows the formation of magnetic nanoparticles. The absorption band at 447 cm^{-1} attributed to tetrahedral and octahedral sites and peak at 3385 cm^{-1} due to the O-H stretching adsorbed on the surface of the Fe_3O_4 nanoparticles [11].

In the case of CV-Fe_3O_4 nanoparticles (curve b in Figure 3); the adsorption of CV is established by the appearance of peaks at 2918 and 2843 cm^{-1} considered to be the stretching vibrations of -CH_3. The appearance of peaks at 1538 and 1630 cm^{-1} are assigned to the C-C

ISSN: 2471-4879

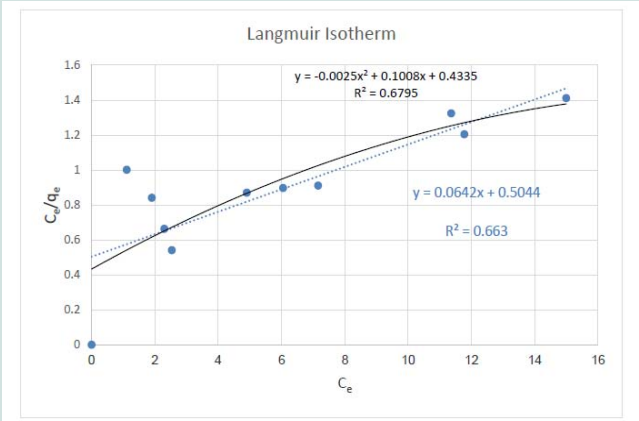

Figure 10: Langmuir adsorption isotherm.

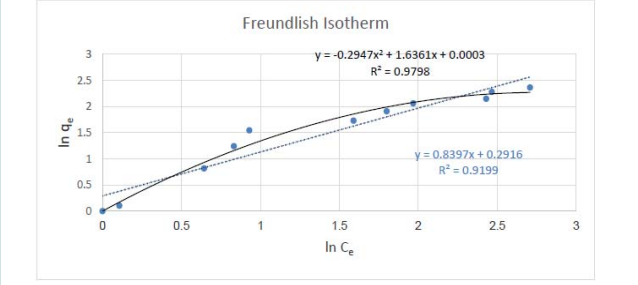

Figure 11: Freundlich adsorption isotherm.

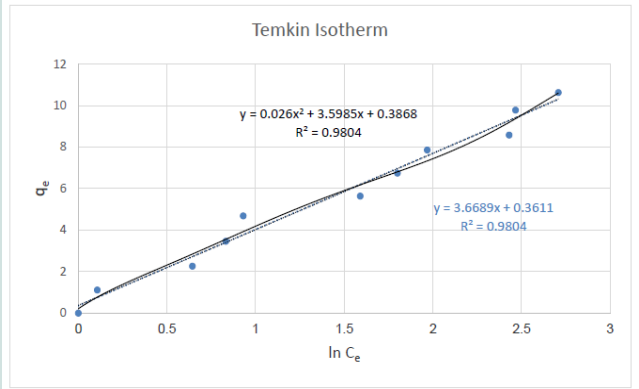

Figure 12: Temkin adsorption isotherm.

stretching vibration of the aromatic (bending vibration).

The appearance of peak at 1025 cm^{-1} (C-N stretch) confirms adsorption of CV (dimethylamino). The observed shift of bands to higher and /or to lower wavelength is taken as a strong evidence for the adsorption process (Figure 3).

Adsorption Parameters

Effect of pH: When the pH of the dye solution increased, the amount of dye adsorbed also increases (Figure 4). The adsorption of cationic dye is promoted due to electrostatic forces of attraction between the negatively charged adsorbent and the positively charged dyes molecules [12,13]. It is noticeabe that high removal efficiency even at neutral pH (74.75%, 89.23% and 92.23%) for concentrations of 50, 25 and 10, respectively.

Proposed mechanism for adsorption: Based on the result obtained from the effect of pH; at high pH, an oxide surface will probably exist and this will increase the negative charge, while with deceasing pH the hydroxide form will instead of oxide form (positive polarization).

ISSN: 2471-4879

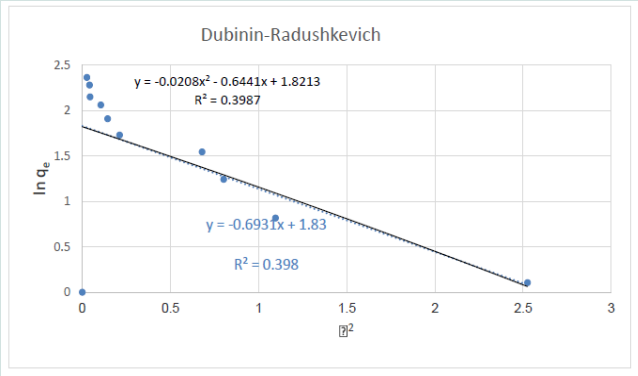

Figure 13: D-R adsorption isotherm.

Figure 14: Pseudo-first order adsorption kinetics of CV onto MNPs.

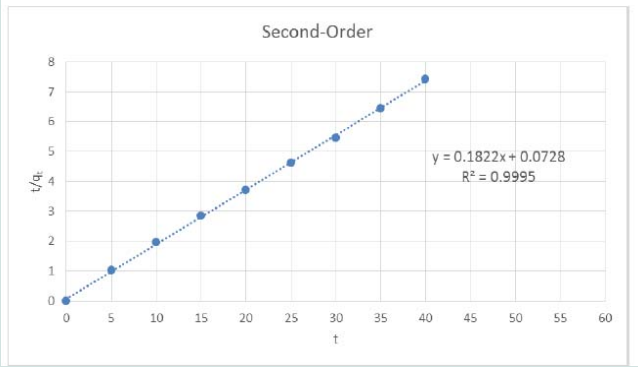

Figure 15: Pseudo-second order adsorption kinetics of CV onto MNPs.

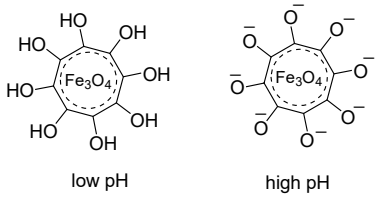

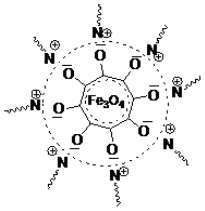

This confirms that the adsorption process is promoted as electrostatic attraction mechanization at higher pH.

ISSN: 2471-4879

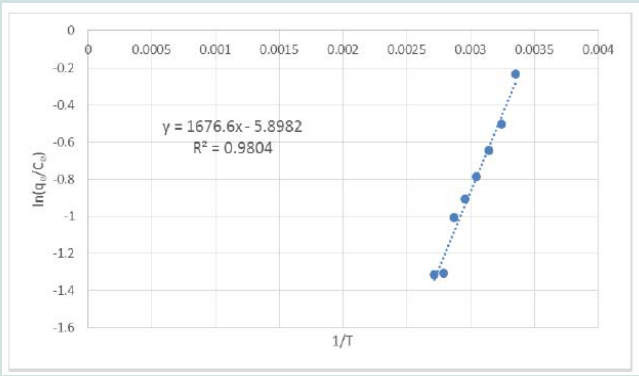

Figure 16: Linear plot of ln qe/Ce versus 1/T.

Effect of time

The influence of the time on the adsorption of CV on MNPs was evaluated to determine the equilibrium time and to investigative the adsorption process (Figure 5). The removal rate (%) increases with time and detects a rapid removal during the first few minutes of contact until the equilibrium state is reached (35 min at r.t.). The uptake ratios (%) obtained after equilibrium are 86.99%, 95.70% and 99.73% for CV adsorption onto MNPs for concentrations of 50 mg/l, 25 mg/l and 10 mg/l, respectively.

Effect of sorbent dose

From Figure 6, the removal efficiency of investigated dye increases rapidly with increasing amount of MNPs. At the same time, further increasing the adsorbent dose leads to a slightly decrease of the removal efficiency. The removal rate (%) decreases with increase in concentration and takes prolonged period to reach equilibrium because of the verity that with increase in dye concentration, there will be increase in contest amongest the dye molecules and the adsorption process will increasingly slowing down [14].

Effect of dye concentration

The effect of the concentration of the dye adsorption process was investigated (10-100 mg l^{-1} at 25 °C and pH 9). The concentration of the dye at λ_{max} was obtained using a standard calibration curve. The adsorption is very rapid in the initial stages of the adsorption until concentration of 50 (higher than 90%) and then decreased for higher concentrations (Figure 7). This can be clarified by a large number of active centers at the starting of adsorption and saturation of these centers on the surface of the adsorbent with attaining equilibrium. The requisite time for reaching the equilibrium increases with increasing the concentration due to the fact that adsorption involves film diffusion and internal diffusion [15].

Effect of temperature

Temperature is a point for the adsorption whether it is an endothermic or exothermic process. The solubility and chemical potential of dye is affected by increasing the temperature. Figure 8 represents the sorption of CV onto MNPs at various temperatures (25 °C to 95 °C) with a fixed initial dye concentrations (10, 25 and 50 mg l^{-1}). With increasing the temperature the rate of adsorption decreases that indicates the adsorption process is exothermic. The decrease in rate of adsorption with increasing temperature, this may be due to when the temperature increased the solubility of dye will be increased.

Adsorption isotherms

The sorption profile of CV was specified over a wide range of equilibrium concentrations (10-100 ppm) as shown in Figure 9.

Adsorption isotherms

Langmuir isotherm: Langmuir equation used is given below:

$$q_e = (q_m\, b\, C_e) / (1+b\, C_e) \quad (1)$$

Where: (C_e; equilibrium concentration of dye), (q_e; the amount of dye adsorbed at equilibrium), (q_m; Langmuir monolayer adsorption capacity (mg/g)), and (b; Langmuir constant (l/mg)). The equation is linearized by different ways to give the next equation:

$$C_e/q_e = 1/(q_m\, b) + C_e/q_m \quad (2)$$

A straight-line plot of C_e/q_e *vs.* C_e (Figure 10) indicated that uptake rate of CV dye occurred on adsorbent (MNPs) homogenous surface by monolayer adsorption without any interaction between adsorbate molecules. The values of b and q_m for the system evaluated from the intercept and slope were 0.127 and 15.57 for CV dye. These values indicate good retention for CV onto MNPs.

The value of adsorption capacity of MNPs was compared with the adsorption capacities of various adsorbents (Table 1). According to that comparison, MNPs have a good adsorption capacity for CV

Freundlich isotherm

It is often used to depict non-specific adsorption that comprises of heterogeneous surfaces.

$$q_e = k_f * C_e^{1/n} \quad (3)$$

The equation is linearized by different ways to give the next equation:

$$ln\, qe = ln\, k_f + (1/n)\, ln\, C_e \quad (4)$$

Where: (k_f; Freundlich coefficients (m/g)) and (n; related to adsorption intensity) were obtained from the slope and the intercep of the linearized Freundlich plots.

The plot of ln C_e versus *ln* q_e of CV in Figure 11 is straight line

ISSN: 2471-4879

Table 1: The adsorption capacities of different adsorbents for crystal violet dye.

Adsorbent	q_e (mg.g^{-1})	Reference
Sagaun sawdust	3.5	Khattri, S., Singh, M. (2012)
agro-industrial wastes	10.44	Parab, H. et.al (2009)
bioadsorbent	4.44-3.99	Khattri, S., Singh, M. (2000)
De-oil soya	5.79	Bennani Karim, A. et.al (2017)
Neem sawdust	3.8	Sarada , B. et.al (2014)
MNPs	15.57	Present work

Table 2: Constants and correlation coefficients for the four isotherms.

Model	Parameter	Linear regression	Nonlinear regression
Langmuir	**q_m (mg/g)**	**15.75**	
	b (l/mg)	0.127	
	R^2	0.663	0.679
	SEE	0.239	0.234
Frundlich	**K_F (mg/g)**	**1.191**	
	1/n	0.84	
	R^2	0.919	0.979
	SEE	0.250	0.125
Temkin	**q_m (mg/g)**	**3.669**	
	t (1/g)	1.103	
	R^2	0.9804	0.980
	SEE	0.523	0.520
Dubinin	D (mol^2/J^2)	0.693	
	q_m (mol/g)	6.234	
	R^2	0.398	0.398
	SEE	0.685	0.950

Table 3: Adsorption dynamic constants (calculated and experimental q_e values obtained at 50 ppm of CV).

C_i (ppm)	q_e Exp. (mg/g)	Pseudo-first order kinetic model			Pseudo-second order kinetic model		
		K_1 (1/min)	q_e Cal. (mg/g)	R^2	K_2 (g/mg min)	q_e Cal. (mg/g)	R^2
50	5.637	0.034	0.691	0.728	0.429	5.488	0.999

Table 4: Thermodynamic parameters for the adsorption of CV (10 ppm) on MNPs.

T (K)	ΔG (KJ/mol)	ΔH (KJ/mol)	ΔS (KJ/mol K)
298	0.6739	- 0.4077	- 13.939
308	0.116		
318	1.655		
328	2.145		
338	2.635		
358	3.616		
368	4.107		

over the entire concentrations of dye in the aqueous phase. The values of $\mathbf{k_f}$ and 1/n computed from the intercept and slope of the plot were equal to 1.191 and 0.84 for CV. The amount of 1/n < 1 indicates that the sorption strength is slightly miniature at lower equilibrium concentration and the isotherm does not predict any saturation of the solid surface of the adsorbent by the adsorbate [16,17].

Temkin isotherm

It assumes that the heat of adsorption of all the molecules in the layer decreases linearly with coverage due to adsorbate species adsorbent interactions, and adsorption is described by a regular distribution of binding energies, up to some maximum binding energy [18].

$$q_e = q_m \, ln \, (t + C_e) \quad (5)$$

The equation is linearized by different ways to give the next equation:

$$q_e = q_m \, ln \, t + q_m \, ln \, C_e \quad (6)$$

Where: (q_e; the concentration of CV removed (mg/g)), (t; the equilibrium binding constant (l/g)) and (q_m; constant related to heat of adsorption (J/mol).

The linear plot of q_e versus ln C_e for both the adsorption system gave good fit for the Temkin isotherm as shown in Figure 12. The computed values of q_m and t from the slope and intercept were equal 3.669 and 1.103 for CV dye, respectively.

Dubinin-Radushkevich isotherm (D-R)

It is used to evaluate the characteristic porosity of the adsorbent and the apparent energy of adsorption. It is illustated by the equation:

ISSN: 2471-4879

$q_e = q_m\, e^{(-D\mathcal{E}2)}$ (7)

The equation is linearized by different ways to give the next equation:

$Ln\ q_e = ln\ q_m - D\mathcal{E}2$ (8)

$\mathcal{E} = RT\ ln\ (1+1/C_e)$ (9)

Where: (q_e; amount of CV adsorbed on MNPs), (q_m; highest adsorption capacity mg/g), (D; constant related to the energy of adsortion ($mol^2\ KJ^2$), (C_e; equilibrium concentration of CV in mg/l) and (ε; RT ln ($1+1/C_e$), which is called as Polanyi Potential).

A plot of ln q_e versus ε^2 as shown in Figure 13 yielding straight line confirms the model. The D-R constant can be specified from the intercept of the straight-line diagram.

Error analysis

To estimate the fit of the adsorption isotherm and isotherm parameters by linear and nonlinear regression, Standard Error of the Estimate function (SEE) was applied. It is the most commonly used error evaluation function and the mathematical form of the SEE can be written as:

$SEE = \sqrt{\Sigma(\dot{y}-y)^2/n-2}$

ẏ: Estimated value

y: Actual value

n: # of values

The isotherm parameters determined by linearization and the nonlinear regression of the Langmuir, Freundlich, Temkin and Dubinin equations, using Standard Error of the Estimate function, together with the correlation coefficient (R^2) and error values, are summarized in Table 2.

The results obtained from the linear and the nonlinear regressions with Standard Error of the Estimate function were compared. It was found that the regression methods revealed that CV adsorption were better fitted to the Freundlich isotherm (nonlinear regression) in terms of the R^2 and error values, because of the higher R^2 values and lower error values than those of other models.

Adsorption Kinetics

The dynamics of the adsorption of CV onto MNPs were inspected using the Lagergren's pseudo-first order (Eq. 10) and pseudo-second order (Eq. 11) equations:

$Log\ (q_e-q_t) = Log\ q_e - k_1 t / 2.303$ (10)

$t / q = 1/ K_2 q_e^2 - [1 / q_e]\ t$ (11)

Where: (q_e and q_t; the amount of dye adsorbed at equilibrium and at any time t, respectively), (k_1; the first-order adsorption rate constant (1/min)), (k_2; the pseudo-second order rate constant (g/mg min)). The K_1 and K_2 have been calculated from the intercept of the corresponding of log (q_e-q_t) versus t as shown in Figure 14 and t/q versus t shown in Figure 15, and are tabulated in Table 3.

The correlation coefficient value (R^2) for the pseudo-second order rate equation was higher than the pseudo-first order rate equation, so through these results, it was assured that the adsorption system pursued the pseudo-second order rate equation.

Thermodynamic Studies

To further understand the effect of temperature the thermodynamic parameters including the change in Gibbs free energy (ΔG, KJ /mol), enthalpy (ΔH, KJ/mol), and entropy (ΔS, KJ/mol K), were used to describing thermodynamic behavior of CV onto MNPs. Thermodynamic equations can be expressed as follow:

$\Delta G = - RT\ ln\ K$ (12)

$K = q_e/C_e$ (13)

$\Delta G = \Delta H - T\Delta S$ (14)

Where: (ΔG; the Gibbs free energy (KJ /mol)), (ΔH; the change in enthalpy (KJ/mol)), (ΔS; the entropy change (KJ/mol K)), (T; the absolute temperature in (K)), (K; the equilibrium constant (1/q)), (R; the universal gas constant (KJ /mol K)), (q_e; the amount of adsorbed dye onto MNPs (mg/g)), and (C_e; the equilibrium concentration of CV in the solution (mg/l)).

The values of the thermodynamic parameters reported in Table 4 were obtained from the linear plot of ln K versus 1/T (Figure 16). The positive value of ΔH indicates the endothermic nature of adsorption. The negative amount of ΔG indicates the spontaneous nature of the adsorption of CV onto MNPs. The positive amount of ΔS shows the increased disorder and randomness at the solid solution interface during the adsorption dye on the adsorbent [19-21] . The magnitude of ΔG, ΔH and ΔS vales indicate that the adsorption of CV onto MNPs is nonspontaneous at high temperature and spontaneous at low temperature. It can be said that the adsorption of CV MNPs is physical adsorption and the forces can be Van deer Waals forces or electrostatic attraction between CV and MNPs surface.

Conclusion

The present study highlights the potential application of iron oxide nanoparticles to remove the crystal violet dye. The adsorption of CV was found to increase with increase in time, decrease temperature, decrease dye concentration and increase pH up to equilibrium amont. It was found the adsorption process of CV on MNPs was exothermic and spontaneous. A pseudo-second order equation well explained the kinetic data and revealed the physisorption.

References

1. Wang S, Boyjoo Y, Choueib A, Zhu ZH (2005) Removal of dyes from aqueous solution usng fly ash and red mud. Water Res 39: 129-138.
2. Vital RK, Saibaba KVN, Shaik KB, Gopinath RA (2016) Dye removal by adsorption: A Review. J Bioremediat Biodegrad 7: 371.
3. Mahmoodi NM, Soltani-Gordefaramarzi S (2016) Dye removal from single and quaternary systems using surface modified nanoparticles: Isotherm and kinetics studiees. Progress in Color, Colorants and Coatings 9: 85-97.
4. Tang R, Dai C, Li C, Liu W, Gao S, et al. (2017) Removal of methylene blue from aqueous solution using agricultural residue walnut shell: equilibrium, kinetic, and thermodynamic studies. J Chem 8404965.
5. Al-Rubayee WT, Abdul-Rasheed OF, Ali NM (2016) Preparation of a modified nanoalumina sorent for the removal of alizarin yellow R and methylene blue dyes fom aqueous solutions. J Chem 4683859.
6. Muntean SG, Nisto MA, Muntean E, Tode A, Ianoş R, et al. (2018) Removal

ISSN: 2471-4879

of colored organic pollutants from wastewaters by magnetite/carbon nanocomposites: single and binary systems. J Chem 2018: 16.

7. Kong L, Gan X, Ahmad ALb, Hamed BH, Evarts ER, et al. (2012) Design and synthesis of magnetic nanoparticles augmented microcapsule with catalytic and magnetic bifuntionalities for dye removal. Chem Engineering J 197: 350-358.
8. Lotfi Zadeh Zhad HR, Aboufazeli F, Sadeghi O, Amani V, Najafi E, et al. (2013) Tris(2-aminoethyl)amine-functionalized F_3O_4 magnetic nanoparticles as a selective sorbent for separation of silver and gold ions in diffrent pHs. J Chem 482793.
9. Simona GM, Maria AN, Eliza M, Anamaria T, Robert I, et al. (2018) Removal of colored organic pollutants from wastewaters by magnetite/nanocomposite: single and binary systems. J Chem 6249821.
10. Abdo NI, Abobakkr SM, Abd El-Wahab AE, El-Deeb NM (2019) Superparamagnetic iron oxide nanoparticles with antimicrobial activities: synthesis and characterization of stable dispersion of Fe_3O_4 in DMSO/citric acid, Adv Sci Eng Med 11: 783-788.
11. Pham XN, Nguyen TP, PhamTN, Tran TTN, Tran TVT (2016) Synthesis and characterization of chitosan-coated magnetite nanoparticles and their application in curcumin drug delivery. Adv Nat Sci: Nanosci Nanotechnol 7: 045010.
12. Muntean SG, Paska O, Coseri S, Simu GM, Grad ME, et al. (2013) Evaluation of a functionalized copolymer adsorbent on direct dyes removal pocess: kinetics and equilibrium studies. J Appl Polym Sci1 27: 4409-4421.
13. Mansour RA, Aboeleneen NM, AbdelMonem NM (2018) Adsorption of cationic dye from aqueous solutions by date pits: Equilibrium, kinetic, thermodynamic studies, and batch adsorber design. Int J Phytoremediation 20: 1062-1074.
14. Nandi BK, Goswami A, Purkait MK (2009) Adsorption characteristics of brilliant green dye on kaolin. J Hazard Mater 161: 387-395.
15. Liu R, Zhang B, Mei D, Zhang H, Liu J (2011) Adsorption of methy violet from aqueous solution by halloysite nanotubes. Desalination 268: 111-116.
16. Farag AB, Soliman MH, Abdel-Rasoul OS, El-Shahawi MS (2007) Sorption characteristics and chromatographic separation of gold (I and II) from silver and base metal ions using polyurethane foams. Analytica Chimica Acta 601: 218-229.
17. Al-Ahmary KM (2009 Retention profile of cadmium and lead ions from aqueous solutions onto some selected local solid sorbents. Journal of Taibah University for Science 2: 52-61.
18. Wang H, Su JQ, Zheng XW, Tian Y, Xiong XJ, et al. (2009) Bacterial decolorization and degradation of the reative dye red 180 by Citrobacter sp. CK3. Int Biodeterioration Biodegradation 63: 395-399.
19. Paska OM, Pacurariu C, Munteon SG (2014) Kinetic and thermodynamic studies of methylene blue biosorption using corn-husk. RSC Advances 4: 62621-62626.
20. Anusha S, Azrina A, Pichiah S, Manickam M (2012) Adsorption of mercury (II) ion from aqueous solution using low-cost activated carbon prepared from mango kernel. Asia-Pacific J Chem Eng 8: 1-10.
21. Vijayalakshmi P, Bal VSS, Thiruvengadaravi KV, Panneerselvam P, Palannichamy M, et al. (2010) Removal of Acid Violet 17 from Aqueous Solutions by Adsorption onto Activated Carbon Prepared from Pistachio Nut Shell. Separation Science and Technology 46: 155-163.